Reversible Chromosome Condensation Induced in *Drosophila* Embryos by Anoxia: Visualization of Interphase Nuclear Organization

VICTORIA E. FOE and BRUCE M. ALBERTS
Department of Biochemistry and Biophysics, University of California, San Francisco, San Francisco, California 94143

ABSTRACT We have studied the morphology of nuclei in *Drosophila* embryos during the syncytial blastoderm stages. Nuclei in living embryos were viewed with differential interference-contrast optics; in addition, both isolated nuclei and fixed preparations of whole embryos were examined after staining with a DNA-specific fluorescent dye. We find that: (a) The nuclear volumes increase dramatically during interphase and then decrease during prophase of each nuclear cycle, with the magnitude of the nuclear volume increase being greatest for those cycles with the shortest interphase. (*b*) Oxygen deprivation of embryos produces a rapid developmental arrest that is reversible upon reaeration. During this arrest, interphase chromosomes condense against the nuclear envelope and the nuclear volumes increase dramatically. In these nuclei, individual chromosomes are clearly visible, and each condensed chromosome can be seen to adhere along its entire length to the inner surface of the swollen nuclear envelope, leaving the lumen of the nucleus devoid of DNA. (c) In each interphase nucleus the chromosomes are oriented in the "telophase configuration," with all centromeres and all telomeres at opposite poles of the nucleus; all nuclei at the embryo periphery (with the exception of the pole cell nuclei) are oriented with their centromeric poles pointing to the embryo exterior.

During its syncytial blastoderm stages, the *Drosophila* embryo is a large single cell containing hundreds of nuclei that divide almost synchronously. For this reason, it provides exceptional material for cytologic studies of the nuclear division cycle. The blastoderm stages with which our study is concerned (cycles 10–14) are represented diagrammatically in Fig. 1, where, according to the terminology of Zalokar and Erk (39), each stage corresponds to one nuclear division cycle. Initially, all the dividing nuclei are located in the egg interior, but during cycle 7, ~80% of these nuclei begin migrating towards the embryo surface (7). Near the start of interphase of cycle 9, a few nuclei reach the surface at the posterior pole of the egg; during cycle 10 these nuclei cellularize to form the primordial germ cells, the "pole cells." Slightly after the start of interphase of cycle 10, the rest of the migrating nuclei reach the egg surface, becoming distributed in a monolayer just under the egg plasma membrane. Once at the surface these nuclei undergo four nearly synchronous divisions as a syncytium (the syncytial blastoderm stages: nuclear cycles 10–13). Cellularization of these nuclei occurs synchronously during the first 60 min (25°C) of interphase 14 (stage 14A in Fig. 1), whereas gastrulation and germ band elongation occur during the remainder of interphase 14 (stage 14B in Fig. 1).

Once the somatic nuclei have reached the egg surface (nuclear cycle 10), they can be visualized clearly in living embryos by differential interference-contrast optics (see Figs. 4 and 5 of reference 7). During the syncytial blastoderm stages, mitotic waves pass rapidly across the embryo surface, and thus the nuclei divide with near synchrony. The duration of each of the syncytial nuclear cycles has been determined, making it possible to stage living embryos to an accuracy of ~±1.5 min (7). In this article, we describe the regular changes in interphase nuclear volume that occur during nuclear cycles 10 through 14. In addition, we report a method for inducing a reversible developmental arrest at any time during this period; during this arrest the chromosomes condense, allowing the arrangement of the chromosomes in each nucleus to be clearly visualized.

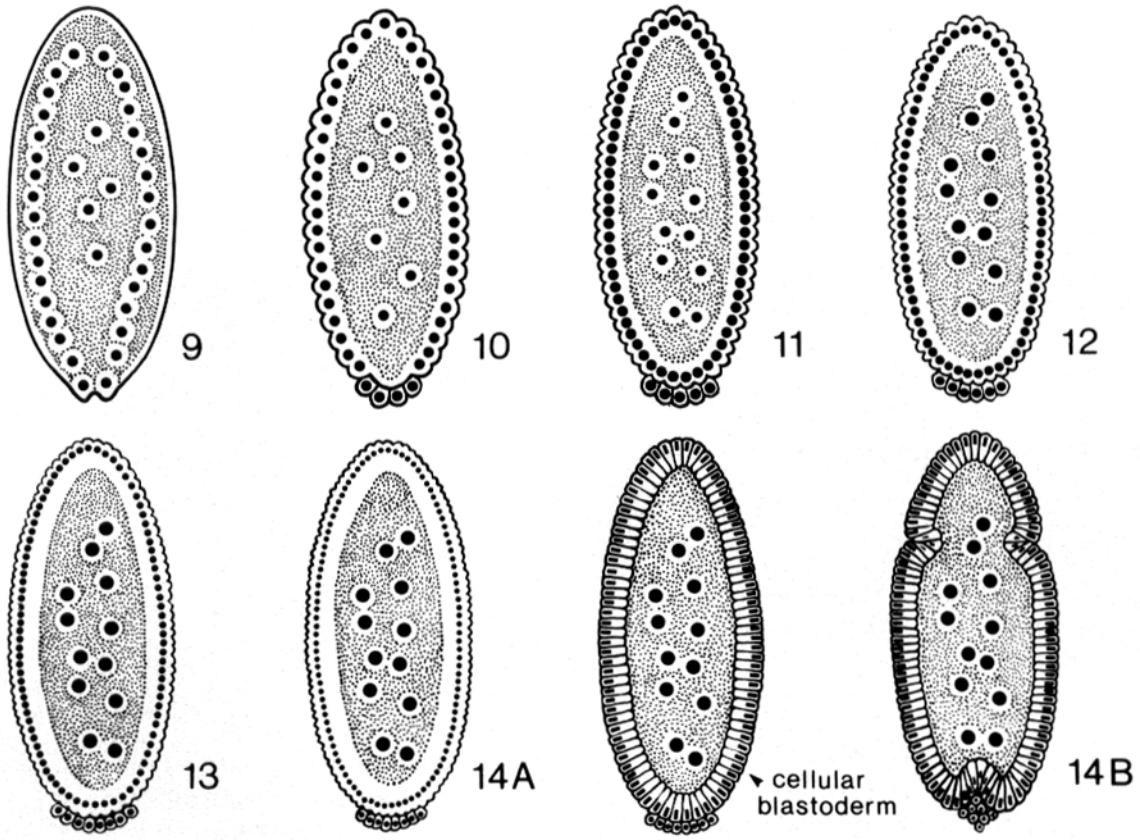

FIGURE 1 Schematic drawing of the pregastrula embryonic stages in *Drosophila melanogaster* (detail of Figure 1 of reference 7). The number beside each embryo, which denotes its developmental stage, is related to the total number of nuclear division cycles that the almost synchronously dividing embryonic nuclei undergo. A stage begins with the start of interphase and ends with the conclusion of mitosis. The stages, each of which corresponds to one complete nuclear division cycle (interphase plus mitosis), are numbered consecutively. Stage 14A is depicted at both early (no cell membranes evident) and late (cellularization just completed) times. Embryos are shown in longitudinal section, with their anterior end up, and nuclei are represented by solid circles. A subset of nuclei do not migrate; those "yolk nuclei" cease dividing after their 10th cycle and become polyploid (see reference 7); their increased ploidy is depicted by solid circles of greater diameter. The average durations of stages (nuclear cycles) 10, 11, 12, 13, and 14 are 8.8 ± 0.6, 9.5 ± 0.7, 12.4 ± 0.9, 21.1 ± 1.5, and >65 min, respectively (25°C; see reference 7). For a more detailed description of these nuclear division cycles, see text and reference 7.

MATERIALS AND METHODS

Collection and High-Magnification Viewing of Live Embryos

Population cages of laying *Drosophila melanogaster* flies were maintained and their eggs harvested, dechorionated, and staged as described by Foe and Alberts (7). Both wild-type fly stocks (Oregon R strain) and In(1) sc^8, y^{31d} sc^8w^a (24) fly stocks were used for this study. Live embryos were mounted in Halocarbon oil (series 11–21 Halocarbon Products Corp., Hackensack, NJ) in an unsealed, covered preparation (see reference 7) and examined with Zeiss Nomarski differential interference-contrast (DIC, Carl Zeiss, Inc., Thornwood, NY)[1] optics (DIC prism in the focal plane of the objective) at 25°C. For studies of nuclear volume changes, staged live embryos visualized through a Planapochromat 63/1.4 oil-immersion objective (Carl Zeiss, Inc.) were photographed at 30-s intervals, and nuclear diameters were measured from projected photographic images. The film used for both DIC and fluorescence photography was Kodak Technical Pan 2415 (Eastman Kodak Co., Rochester, NY).

Effect of Anoxia on Viability

About 3 g of a mixture of 0–4.5-h-old embryos were dechorionated and placed in a solution of 0.7% NaCl, 0.04% Triton X-100 (7). For studies of normal development, a sample of embryos was immediately removed to an open petri dish to avoid any inadvertent influence of anoxia. Intentional developmental arrest was induced in the remaining embryos by transferring these embryos to a bottle containing NaCl-Triton X-100 medium that had been degassed under vacuum. The bottle was then topped up with argon, sealed shut, and maintained at 25°C. After each designated interval, an aliquot of embryos was removed and returned to a normally aerated saline medium, the remaining embryos being resealed under argon. From each aliquot, 200 normal-appearing embryos of each designated stage were selected under a dissecting microscope. This selection required <10 min and was therefore complete before the arrested embryos had resumed development (see Table 1). After their removal from anoxic conditions the staged embryos were kept in open petri dishes containing nondegassed NaCl-Triton X-100 solution. Batches of no more than ~200 embryos were maintained in each petri dish (5 cm diam) to avoid oxygen deprivation by overcrowding. These embryos were scored 30 h later for viability as described in the legend to Fig. 3.

Kinetics of Anoxic Arrest and Recovery

To study the kinetics of arrest, a single embryo in NaCl-Triton X-100 solution was drawn into a graduated 5-μl micropipette (Micropet No. 4614 from Clay Adams, Div. of Becton, Dickinson & Co., Parsippany, NY). A length corresponding to a 1-μl volume of this pipette, with the embryo approximately equidistant from each end, was broken off and placed in the bottom of a petri dish of NaCl-Triton solution at 25°C. The immersed capillary tubing containing the embryo and salt solution was observed with a dissecting microscope (×120) to monitor the time required for development to cease. To study the kinetics of recovery from anoxia, the embryo was expelled from the capillary tube into normally aerated medium and the time taken to resume development was noted.

[1] *Abbreviation used in this paper:* DIC, differential interference-contrast (optics).

Treatment of Embryos before Fixation

CONTROL EMBRYOS: Live dechorinated embryos in NaCl-Triton X-100 solution at 25°C were staged as described previously (7). Squashed-embryo preparations were then made of individually staged embryos.

ANOXIC EMBRYOS: Single embryos were rendered anoxic in capillary tubing as described above. To obtain embryos arrested in cycle 10, live cycle 9 embryos were selected (see reference 7), placed in a capillary tube and monitored under a dissecting microscope to determine in which nuclear cycle developmental arrest occurs. Since it takes ~10 min (at 25°C) for development to cease (see Table I), and cycle 9 is ~10 min long (at 25°C [7]), most embryos arrested at cycle 10. The precise phase of the nuclear cycle at which the embryos had arrested was inferred from the nuclear morphology observed in each preparation, as described in Results. Unless otherwise stated, squashed-embryo preparations were made from individual embryos that had been kept in an arrested state for 30–180 min.

HEAT-SHOCKED EMBRYOS: Dechorinated embryos in NaCl-Triton X-100 solution at 25°C were transferred by pipette into the same medium at 35–37°C or at 40–42°C for a defined interval. For recovery studies, these heat-shocked embryos were transferred back into the same medium at 25°C. In all cases, nuclear morphology was studied in squashed-embryo preparations.

Fixation and Staining of Embryos for Fluorescence Microscopy

SQUASHED-EMBRYO PREPARATIONS: Selected live embryos were transferred by pipette onto a glass slide, blotted free of the NaCl-Triton solution, and covered with 3–6 μl of a buffered solution of salts designated below as buffer AM (see reference 7) that also contained 1% formaldehyde and 10 μg/ml of the fluorescent DNA-specific dye Hoechst 33258. (The formaldehyde was from a freshly heated [5 min at 100°C] formalin solution, and the dye was obtained from the American Hoechst Corp., Somerville, NJ.) Squashes were prepared directly in this fixation medium by gently lowering an 18-mm² coverslip onto the embryo. Lateral movement of the coverslip was avoided to prevent shearing. The preparation was allowed to sit at room temperature for ~5 min. It was then either sealed with nail varnish and photographed in the following 30 min, or converted to a more permanent preparation by mounting in glycerol (J. Sedat, unpublished protocol). In the latter case, the slide was flooded with excess buffer AM and the coverslip was removed by flotation; the slide was then shaken free of excess buffer, and a drop of 100% glycerol and a new coverslip were immediately placed on the sample. Mounting in glycerol preserves nuclear morphology for days.

All of the nuclei displayed in this publication were from fresh squash preparations, without glycerol, and the nuclei are displayed at the same magnification to facilitate comparison.

WHOLE-EMBRYO PREPARATIONS: Timed collections from 0.5 to 2.5 g of dechorionated embryos were placed in a solution of 0.7% NaCl, 0.4% Triton X-100 (7). For studies of normal morphology, the collected embryos were fixed immediately to avoid any inadvertent influence of anoxia. For studies of anoxic embryos, the embryos were transferred to a bottle of the same solution that had been degassed under vacuum. The bottle was then topped up with argon and sealed shut for 2–6 h. Both normal and arrested embryos were fixed and stained using the protocol of Mitchison and Sedat (29) and staged by counting the number of surface nuclei per unit area, as described previously (7). In these fixed and stained whole embryos (suspended in 100% glycerol), nuclei of all stages shrink to about two-thirds of the diameter observed in DIC images of live embryos. For Table II, the diameters of all nuclei were multiplied by 1.5 to correct them to in vivo values.

All Hoechst 33258-stained preparations were observed by fluorescence microscopy, using a Zeiss Epi-illumination system with the Zeiss 01 filter set (excitation beam of 365 nm split with a dichroic mirror at 420 nm) plus a long pass 410 nm barrier filter and a Neofluor 100/1.3 oil-immersion objective. The fluorescence micrographs are displayed at exposures optimal for revealing morphologic detail and do not necessarily portray the relative fluorescence of the various nuclei.

RESULTS

Nuclear Volumes Expand and Contract Rapidly during Each Division Cycle

Previous studies of fixed *Drosophila* embryos have indicated that the nuclei increase in volume during the course of each interphase (7, 31) and that the average size of the syncytial blastoderm nucleus decreases with increasing developmental stage (39). During cycles 10 through 13, the time course of these changes in nuclear diameter can be readily measured from successive DIC micrographs of living embryos. In Fig. 2 we have compiled data from measurements made on 11 embryos. In Fig. 2*A*, nuclear diameters are plotted as a function of developmental age; the nuclear volumes computed from these data are similarly plotted in Fig. 2*B*. During each interphase the size of a nucleus increases to a peak value and then declines, reaching its minimum value just before the nuclear envelope becomes indistinct during mitosis. The nuclear volumes at the beginning of interphase are about the same during each cycle. However, the shorter the cycle the more rapid and greater is the volume increase during interphase. For example, nuclei in cycle 10 (nuclear cycle time of ~9 min) require only 3 min to attain their peak sixfold volume increase, whereas nuclei in cycle 13 (nuclear cycle time of ~21 min) require ~10 min to achieve their threefold volume increase (Fig. 2*B*).

As the cell plasma membranes form around the nuclei during the first half of cycle 14, the nuclei change shape, becoming roughly cylindrical instead of spherical. Both this shape change and the increased light scattering associated with the presence of the newly forming cell membranes make it difficult to determine nuclear volumes in living embryos during much of this cycle. However Fullilove and Jacobson (9) have reported a maximum nuclear volume increase of 2.5-fold during this cycle from an analysis of sectioned material.

The relative areas under the curves displayed in Fig. 2*B* for cycles 10, 11, 12, and 13 are 1.00, 0.93, 0.97 and 1.59, respectively.

Oxygen Deprivation of Drosophila Embryos Causes a Reversible Developmental Arrest

When embryos are overcrowded in open petri dishes or sealed under coverslips, they undergo a developmental arrest. This arrest was systematically studied in embryos intentionally deprived of oxygen by a sudden transfer to degassed medium. Under the conditions used (see Materials and Methods), all further nuclear division rapidly ceases, and dramatic changes in the nuclear organization occur (see below). Embryos can be maintained in this growth-arrested state for extended periods with no detectable change in their appearance. On return to oxygenated medium, the nuclei in these embryos can recommence their divisions and produce normal larvae.

Table I lists the times required for single embryos held in capillary tubes in 1 μl of normally aerated saline solution to exhaust their oxygen supply and undergo arrest. Also listed is the time required to resume morphogenetic movements once the arrested embryos are returned to an aerated environment. Embryonic development arrests after 5–10 min in such a capillary tube, and it recommences ~10 min after a return to normally aerated medium.

In Fig. 3 the viability of embryos after oxygen deprivation is shown. Older embryos can be maintained in an arrested state for longer periods than young ones without a major loss of viability. Thus, for example, stage 15 embryos show a nearly normal survival upon return to oxygenated medium after 36 h of arrest, whereas only about half of the stage 9–13 embryos develop normally after 5 h of arrest.

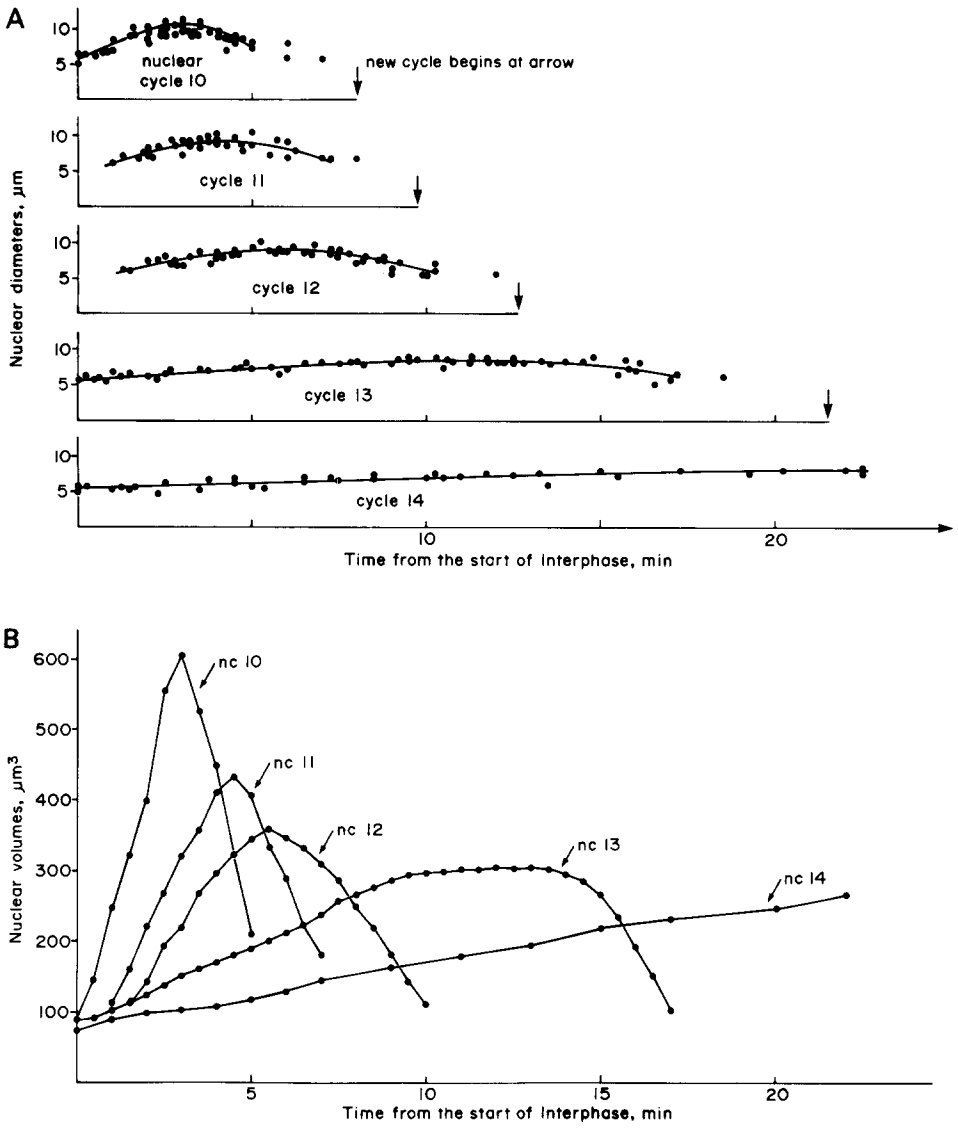

FIGURE 2 Plots of changes in nuclear diameter and volume observed in living embryos during nuclear cycles 10 through 13 and during the first part of cycle 14. (*A*) Nuclear diameters (ordinate) are plotted against the time (at 25°C) from the start of each nuclear cycle (determined as the time when the anterior somatic buds first protrude; see reference 7). Each cycle is plotted separately. The average time at which one cycle terminates and the next cycle begins is indicated by an arrow on the abscissa. The gaps in collection of data points during each cycle correspond to the mitotic period in each cycle, defined as the period during which the nuclear contours become too indistinct to measure. Also, nuclear dimensions were determined for only the early part of cycle 14, when nuclear elongation and cellularization were not so advanced as to interfere with measurements (cycle 14 is >65 min long). Each data point represents a diameter obtained from averaging maximum and minimum diameters of two adjacent nuclei in an embryo. All nuclei followed were at the anterior tip of the embryo, and the data from 11 different embryos were compiled. (*B*) Nuclear volumes during nuclear cycles 10 through 14 (calculated from the data in *A*) are plotted against the time from the start of interphase in each cycle. Data for all five cycles are superimposed on the same axes, in order to facilitate their comparison.

Oxygen Deprivation of Drosophila Embryos Causes the Nuclei To Swell and the Chromosomes to Condense Prematurely onto the Inner Surface of an Enlarged Nuclear Envelope

Nuclear morphology can be studied in whole fixed embryos that have been stained with a DNA-specific fluorescent dye; in these preparations nuclear morphology can be compared across the entire embryo. However, nuclear visibility is improved in squash preparations made from live embryos as described in Materials and Methods. We have used both whole mounts and squashed-embryo preparations to examine the morphology of the arrested embryonic nuclei. We find that the metaphase chromosomes of normal and arrested embryos are indistinguishable, whereas the organization of the chromatin changes drastically in embryos arrested in most other phases of the division cycle; when a nuclear envelope is present, all of the chromatin is displaced from the nuclear lumen onto the inner surface of the nuclear envelope, where it becomes highly condensed. Although presumably caused by a different mechanism, this condensed chromatin resembles the "prematurely condensed" chromosomes created by fusing mammalian interphase cells with mitotic cells (20). By comparing chromosome morphology with that seen in these fused mammalian cells, we can classify the *Drosophila* embryos as being arrested in G_1, S, G_2, or prophase. In Fig. 4, *A–C* are displayed the different types of nuclei observed in the arrested cycle 10 embryos. For comparison, the equivalent phases of normal cycle 10 nuclei are identically displayed in Fig. 5. All of the nuclei in Figs. 4 and 5 are displayed at the same magnification and each nucleus is shown at three different planes of focus to reveal the three-dimensional distribution of its chromatin.

In both Figs. 4 and 5, the nuclei labeled *A* and *B* represent two successive stages of cycle 10 interphase, whereas the nuclei labeled *C* are in prophase. Thus, it is evident that oxygen deprivation has caused both the interphase and the prophase nuclei to swell, although prophase nuclei generally swell more than interphase nuclei. Furthermore, whereas the normal interphase nuclei contain DNA throughout the nuclear lumen (see midsectional view in Fig. 5, *A* and *B*), the oxygen depri-

vation causes all of this DNA to condense against the nuclear envelope, leaving the inside of the nucleus essentially free of DNA (see midsectional view in Fig. 4, *A* and *B*). Similarly, the condensed chromosomes of normal prophase nuclei appear not to be tied to the nuclear envelope throughout their entire length, since they also occupy the nuclear lumen (midsectional view of Fig. 5*C*). In contrast, in prophase nuclei of anoxic embryos, the lumen is free of DNA (midsectional view of Fig. 4*C*), because the chromosomes are closely applied to the nuclear envelope (top and bottom views of Fig. 4*C*).

In nuclei arrested by anoxia in early interphase, the chromatin on the nuclear envelope is not organized into discrete linear chromosomes (Fig. 4*A*); we interpret this to mean that these nuclei have been arrested in S phase, since a similar "fragmented" chromosome morphology is observed when mammalian nuclei active in DNA synthesis are prematurely condensed (20, 32). In contrast, the chromatin of nuclei arrested in late interphase condenses into long discrete chromosomes (Fig. 4*B*). These are thick chromosomes, similar in width to normal prophase chromosomes (compare Fig. 4*B* with Fig. 5*C*), suggesting that they represent chromosomes that were in the G_2 phase of the nuclear cycle. These G_2 chromosomes have a distinctly banded morphology. Nuclei inferred to have been arrested in prophase are similarly organized, but the chromosomes are shorter, more intensely fluorescent and generally appear less banded (Fig. 4*C*). In some of the arrested late prophase nuclei, the very much shortened chromosomes are conspicuously double (not shown).

The thin, single chromosomes that are typically produced when G_1 nuclei are prematurely condensed during cell fusion experiments (20) have not been observed in arrested cycle 10 embryos. Thus, we suspect that in early *Drosophila* embryos, during the rapid nuclear cycles that precede cycle 14, the nuclei proceed directly from telophase into S phase without an intervening G_1 phase.

To ascertain whether oxygen deprivation can cause embryos to arrest at any point in the nuclear cycle, we examined large numbers of embryos arrested in cycle 10 and determined the proportion of embryos blocked in interphase, prophase, prometaphase, metaphase, anaphase, and telophase. For comparison, a similar analysis of cycle phase was carried out on a random sample of normal embryos. Data comparing the relative number of cycle 10 nuclei in each phase of the nuclear division cycle before and after oxygen deprivation is presented in Table II. These data indicate that oxygen deprivation arrests nuclei equally in all phases of the cycle, with the exception that it allows prometaphase nuclei to reach metaphase, and anaphase nuclei to progress to telophase (see legend to Table II).

TABLE I

Analysis of the Time Required for the Onset of Developmental Arrest Caused by Oxygen Deprivation and for the Recovery after Reoxygenation

Embryos tested	Stage	Time lag before arrest	Arrest duration	Time lag before recovery
n		*min*	*h*	*min*
7	Late 14	4 ± 3	3-7	11 ± 3
3	Late 14	5 ± 1	20-23	10 ± 3
10	Early 10	9 ± 4	1-3	11 ± 5

The kinetics of embryo arrest and recovery from oxygen deprivation were studied on individual embryos that were rendered anoxic in glass capillaries, as described in Materials and Methods. We have tabulated the time required before visual morphogenetic movements ceased in each oxygen-deprived embryo, and the time required before morphogenetic movements resumed after returning each embryo to aerated medium.

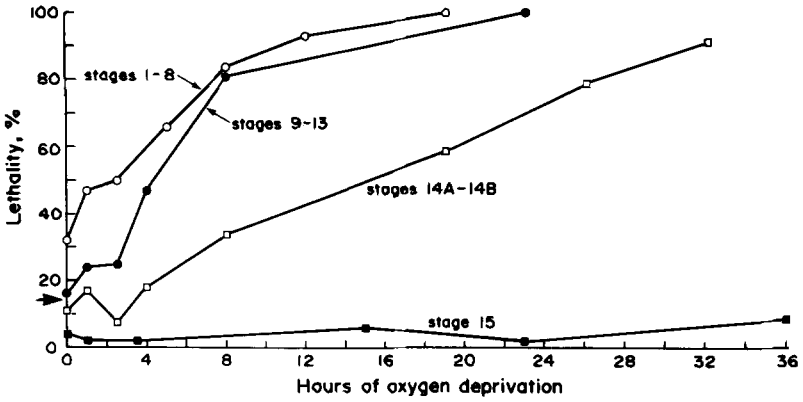

FIGURE 3 Graph showing the mortality of embryos after defined periods of oxygen deprivation. For this study, a large number of 0-4.5-h old dechorionated embryos were arrested by being placed in a nonaerated saline medium (see Materials and Methods). At designated intervals, aliquots of embryos were removed and placed in a normally aerated medium; these embryos were left to develop at 20-25°C and were scored 30 h later. Embryos were scored as viable if they had hatched into normal-appearing mobile larvae. The remainder, which were all scored as lethals, displayed a considerable range of morphologies. A few were normal-appearing embryos that for some reason did not hatch. In most cases, conspicuously deformed larvae or masses of contractile but disorganized tissue developed. Some embryos that arrested at precellular stages developed large noncellularized areas. In only ~5% of the cases did embryos remain at the developmental stage at which they had been arrested. The percentage of lethality after anoxic arrest of specific duration is denoted for embryos arrested during cycle 1-8 with open circles, for embryos arrested between cycles 9-13 with closed circles, for embryos arrested in cycle 14 with open squares, and for embryos arrested in cycle 15 with closed squares. The embryos denoted as cycle 15 embryos were arrested at the late germband extension stage; our studies show that at this stage most nuclei have begun their 15th nuclear cycle (V. Foe, unpublished observations). Each symbol represents data from a sample of 200 embryos. The arrow on the graph ordinate denotes the percentage of lethality of a sample of 200 embryos that were harvested using our usual methods and left to develop without dechorionation in a normally aerated NaCl-Triton solution. Dechorionated stage 9-13 and stage 14 embryos have about the same percentage of lethality as the nondechorionated embryos when none of these are oxygen deprived; however, the lethality is greater after dechorionation for non-oxygen-deprived stage 1-8 embryos (see graph). Thus, some of these younger embryos are damaged during dechorionation, perhaps because newly laid eggs are more permeable than older ones to the Chlorox used for dechorionation. The percentage of lethality of non-oxygen-deprived, dechorionated, stage 15 embryos is below that for the bulk population of nondechorionated embryos, presumably because the selection of cycle 15 embryos excludes many abnormal embryos that would ordinarily have died during earlier stages.

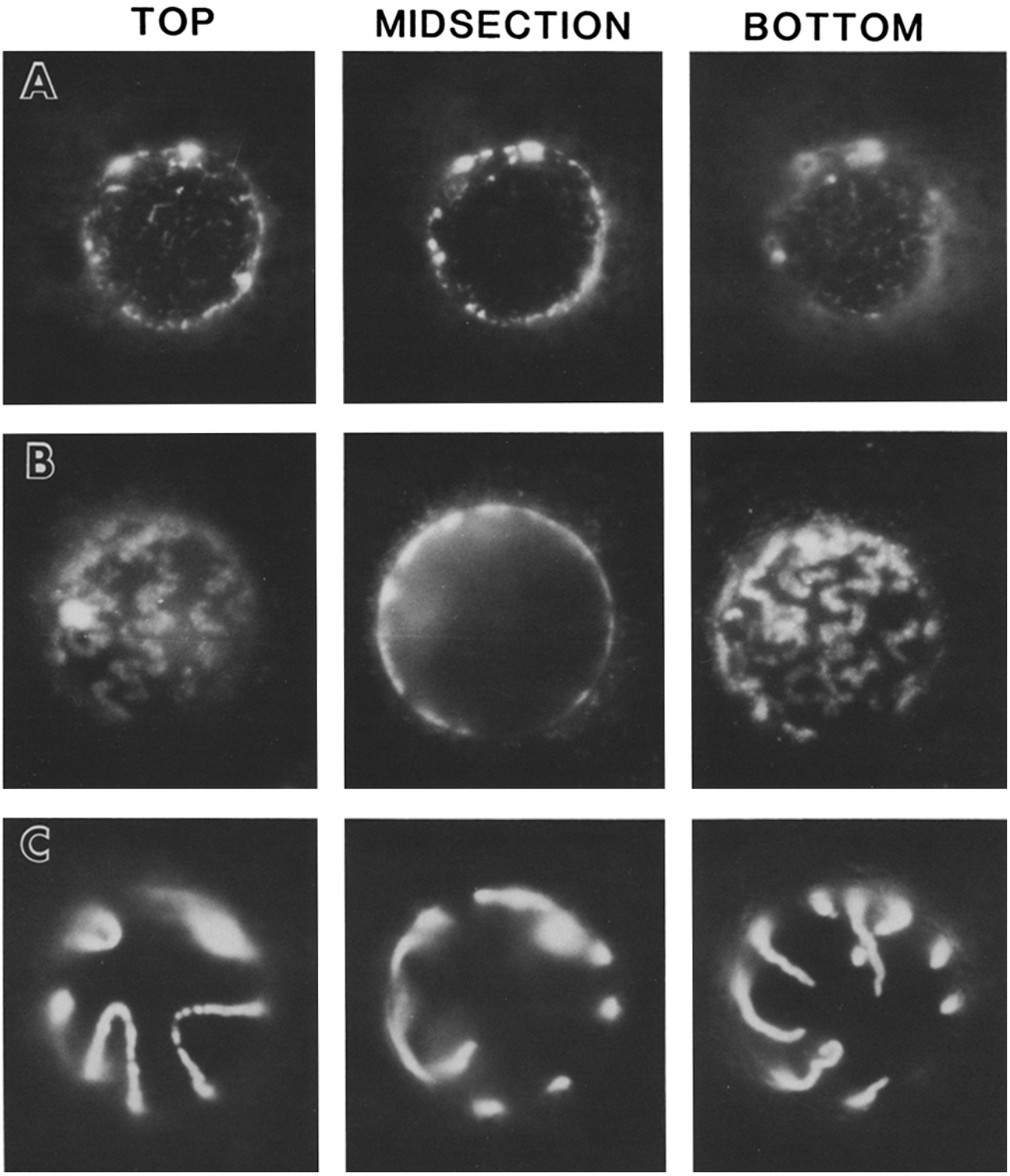

FIGURE 4 Optical sections of cycle 10 interphase nuclei from embryos arrested by oxygen deprivation. These nuclei were photographed in squashed-embryo preparations made from prestaged oxygen-deprived embryos (see Materials and Methods). The phase of their nuclei was inferred from their chromatin morphology, as described in the text. In photographing each nucleus we changed the focal plane to obtain photographs of the top surface (*left*), a midsection (central panels), and the bottom surface (right). The nucleus displayed in *A* is inferred to represent the arrested state of an early interphase (S phase) nucleus and that in *B* an arrested late interphase (G_2 phase) nucleus; more fluorescent chromatin is detected in the G_2 than in the earliest S phase nucleus, presumably because considerable DNA replication has occurred. *C* shows what is inferred to be an arrested prophase nucleus. The chromosome centromeres occur together at one nuclear pole (*left*), whereas the telomeres are at the opposite pole (*right*). A more detailed description of the morphology of these nuclei is presented in the text. In a very small percentage of anoxically arrested, early-to-mid-interphase nuclei, we have observed one or two fluorescent strands extending across the otherwise DNA-free nuclear lumen; this morphology is much more common in heat-shocked nuclei (see text). × 2,600.

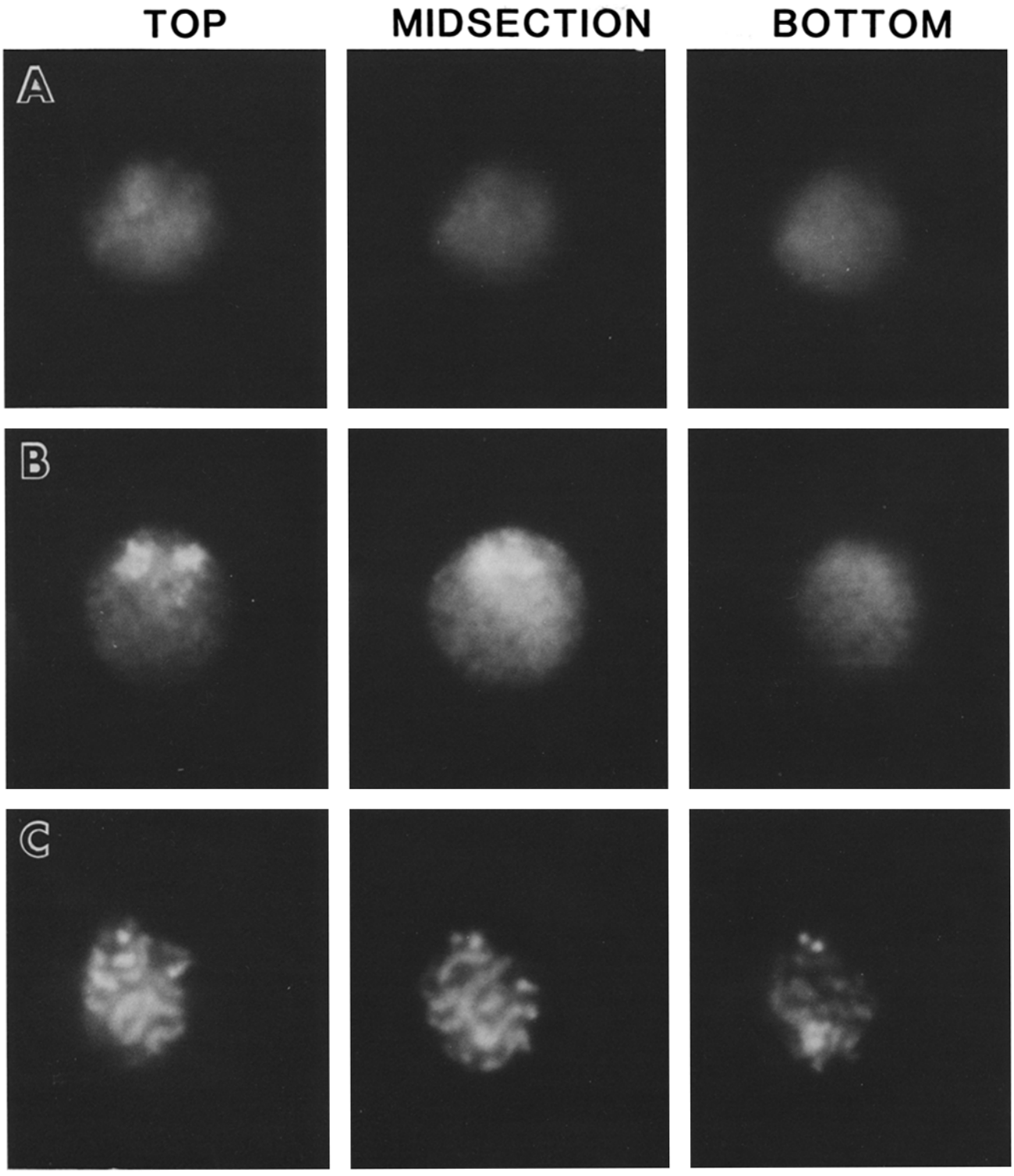

FIGURE 5 Optical sections of normal interphase and prophase nuclei from cycle 10 embryos. These nuclei were from squashed-embryo preparations made from prestaged live embryos (see Materials and Methods). The nucleus shown in *A* is in early interphase (0–2 min), *B* is in mid-to-late interphase (2–4 min), and *C* is in prophase (5–6 min); all times are measured from the start of interphase of cycle 10. In these photographs the nuclei are oriented with the pole that displays the most intense fluorescence in focus on the left and, when not centered over the nucleus, toward the top of the page. For example, two areas of intense fluorescence are apparent in the lefthand panel of *B*, facing the top of the page. Our studies indicate that the nuclear region of most intense fluorescence corresponds to the centromeric pole in the wild-type nucleus (see text); thus the nuclei in Figs. 4 and 5 are displayed in similar orientations. A detailed discussion of the morphology of normal cycle 10 nuclei is presented in the text. × 2,600.

TABLE II

Comparison of the Distribution of Embryos in Different Phases of Nuclear Cycle 10 in Normal and Oxygen-depleted Embryos

	Cycle phase in normal embryos					
	Interphase	Prophase	Prometaphase	Metaphase	Anaphase	Telophase
Frequency of occurrence (%)	47	5	19	12	11	5
Nuclear diameter (μm)	5–11	8	—	—	—	5
	Cycle phase in oxygen-depleted embryos					
	Interphase	Prophase	Prometaphase	Metaphase	Anaphase	Telophase
Frequency of occurrence (%)	40	14	None	29	None	17
Nuclear diameter (μm)	6–15	15	—	—	—	6

The percentage of embryos in each of the different phases of nuclear cycle 10 was determined by analyzing the fluorescent images of a sample of normal embryos 0.5–2.5 h old that had been fixed and stained immediately after collection (see Materials and Methods). An identical analysis was also carried out on a sample of embryos of the same age that were fixed and stained after 3 h of oxygen deprivation. For each preparation, a large sample of embryos was placed on a slide and data on nuclear morphology and nuclear diameter were collected on all of the cycle 10 embryos observed. Cycle 10 embryos were identified by their characteristic number of surface nuclei per unit area (see reference 7). A total of 57 normal cycle 10 embryos and 48 oxygen-deprived cycle 10 embryos were analyzed.

Normal prophase nuclei are defined here as those with a discrete spherical nuclear boundary and condensed chromosomes that have not yet begun to move to a metaphase plate. As judged by a distinct, spherical boundary visible with both phase and DIC optics, a portion of the nuclear envelope persists in these embryos after the chromosomes begin to become oriented on the spindle equator; this boundary gradually disappears as the chromosomes reach their final metaphase configuration. An electron microscopic analysis carried out on these same embryonic stages by Stafstrom and Staehelin (34) suggests that, except near the spindle poles, the nuclear envelope remains largely intact throughout mitosis. However, the nuclear pores begin to disappear from the nuclear envelope during prometaphase and only reappear in this envelope at the beginning of the next interphase (34). We assume that the loss of visibility of the nuclear boundary in the light microscope (see also Figs. 4 and 5 of reference 7) correlates with the loss of nuclear pores detected in the electron microscope. Thus, in our analyses, nuclei that still retain a discrete spherical boundary but whose chromosomes have begun alignment on the spindle are designated as prometaphase, and nuclei with no visible nuclear boundary and with their chromosomes fully aligned on a metaphase plate are designated as metaphase.

Note that no prometaphase nuclei and over twice as many metaphase nuclei are found in the anoxic as compared with the normal embryos. Likewise, none of the anoxic embryos is in early anaphase and there is a threefold increase in the normal proportion of late anaphase and telophase nuclei. Thus, oxygen deprivation does not prevent nuclei in prometaphase from advancing to metaphase, or nuclei in early anaphase from proceeding towards telophase. Nuclei seem to be arrested randomly in all other phases of the cycle. In the anoxic sample, the apparent increase in "prophase" nuclei at the expense of "interphase" nuclei is due to the scoring of some late G_2 nuclei as prophase; in these embryos there is a continuum of chromosome morphologies between G_2 and prophase, making this designation somewhat arbitrary.

In a separate study, the diameters of nuclei in embryos in cycles 10, 11, 12, and 13 were compared. Using an eyepiece reticule, we made size measurements from the preparations of both normal and oxygen-deprived fixed and stained whole embryos described above. We examined a random sample of 67 normal embryos and 121 arrested embryos, staging them by their number of surface nuclei per unit area (7). The amount of swelling observed in the nuclei of anoxic embryos was found to be stage-specific: when corrected to in vivo values (see Materials and Methods), the maximum diameters observed in the arrested nuclei of cycle 10, 11, 12 and 13 embryos were 15.0, 14.0, 12.7, and 11.3 μm, respectively (compared with normal maximum interphase diameters of ~10.9, 10.0, 9.0 and 7.8 μm, respectively; see Fig. 2). Nuclear diameters during different phases of cycle 10 are displayed in the table.

During the Syncytial Blastoderm Stages, the Chromosomes of the Interphase Nucleus Are Oriented with All the Centromeres Facing the Exterior of the Embryo

Individual chromosomes are especially clearly visualized in the nuclei of embryos arrested by anoxia in late interphase or prophase of cycles 10 or 11, because these nuclei swell more than those of later nuclear stages (see data in legend to Table II). In these nuclei a full diploid complement of eight separate chromosomes is seen. An example showing the complete set of chromosomes in a cycle 10 nucleus is displayed in Fig. 6 (see also Fig. 7*B*). As noted above, the bipartite nature of each prophase chromosome is clearly visible in some late prophase nuclei.

In the nuclei from arrested embryos, such as those shown in Figs. 4*C* and 6, the prophase chromosomes can be seen to be positioned in a polarized fashion, with the centromeres at one pole (left panels) and the telomeres near the opposite pole (right panels) of the nucleus. Inspection of many nuclei reveal that this is by far the most commonly observed orientation of chromosomes in interphase and prophase nuclei of cycles 10–13. However, occasional nuclei were found in which individual chromosomes occupy other orientations. For example, in the nucleus displayed in Fig. 6, the small dotlike fourth chromosomes occupy their usual position near the centromeric pole. In contrast, in the otherwise similar nucleus shown in Fig. 4*C* the fourth chromosomes are not present at this location. The polarized chromosomal orientation is abruptly lost at prometaphase, when the chromosomes begin their interaction with the mitotic spindle.

To determine the orientation of the chromosomes in the intact organism, we have examined stained whole embryos that have been arrested by oxygen deprivation in prophase of nuclear cycles 10 through 13. Throughout this period of syncytial development, the chromosomes in the somatic nuclei at the periphery of the embryo are oriented with their centromeres facing the exterior and their telomeres facing the yolk in the interior of the embryo. Two examples are presented in Fig. 7. The plane of focus in Fig. 7*A* is on the interior nuclear faces and shows the clustered telomeric ends of the chromosomes. The plane of focus in Fig. 7*B* is on the midsection at each nucleus, and shows the oriented chromosome arms in cross section.

The pronounced orientation of the chromosomes in the embryonic nuclei revealed by oxygen deprivation apparently reflects a polarity that also exists in the normal embryo. For example, examination of fixed and stained nonanoxic cycle 10–13 embryos reveals that, during mid-to-late interphase, two large and highly fluorescent DNA masses occur in all nuclei of half of the embryos (see, for example, left panel of Fig. 5*B*). From our studies of mutant In(1)sc^8 embryos (see below) we infer that each of these masses represents the centromere-proximal heterochromatin of an acrocentric X chromosome. Since only the nuclei of female embryos have two X chromosomes, embryos whose nuclei resemble that shown in Fig. 5*B* are presumably female. (The more complex

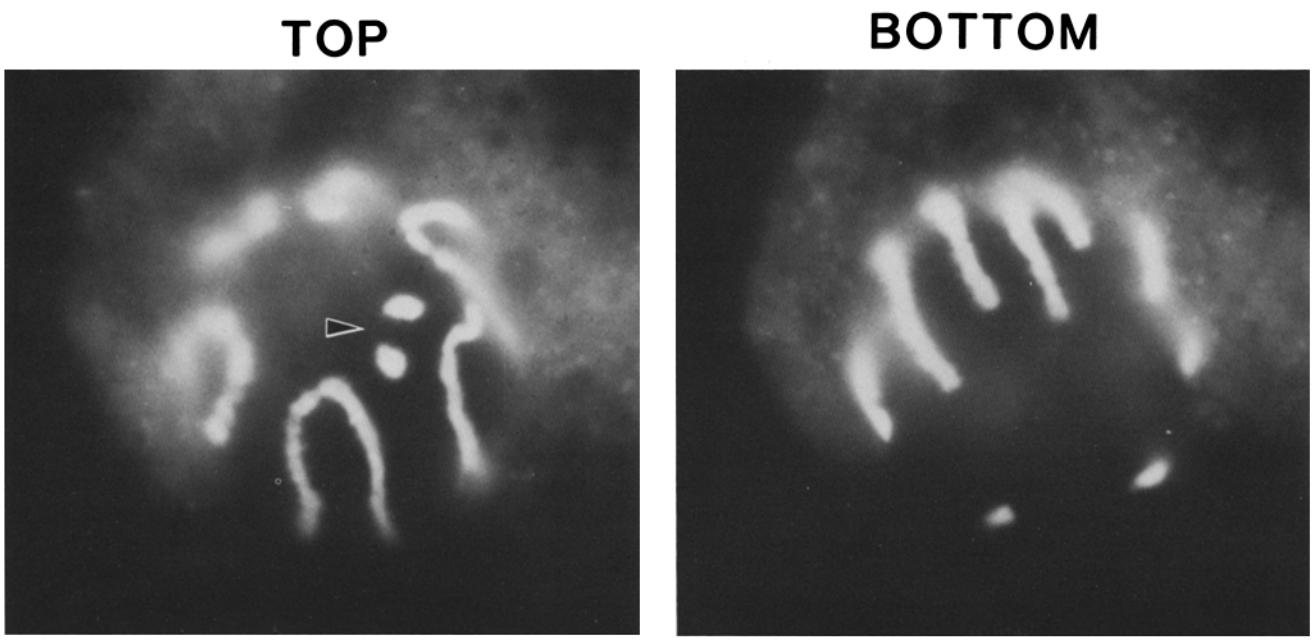

FIGURE 6 A prophase nucleus from an oxygen-deprived cycle 10 embryo. On the left, the plane of focus is on the nuclear pole that contains the centromeres of the chromosomes. The two dotlike fourth chromosomes are conspicuous at this pole (arrowhead). In total, eight chromosomes (including the two fourth chromosomes) are visible at the centromeric pole. On the right, the plane of focus is on the nuclear pole that contains the chromosome telomeres. × 2,600.

organization of the heterochromatic masses in interphase nuclei of male embryos, which carry one X chromosome and a Y chromosome composed of many heterochromatic parts.)[2] In fixed, whole embryo preparations of nonanoxic embryos, such as that displayed in Fig. 8*A*, the bright-staining regions of the two X chromosomes in the female embryos are seen to be located at the exterior-facing pole of each nucleus (labeled TOP), with no comparable fluorescence at the opposite pole (labeled BOTTOM).

We have also examined mid-to-late interphase nuclei in cycle 10–13 embryos that carry rearranged, instead of normal, X chromosomes. In embryos carrying the rearrangement In(1)sc^8, the DNA of the heterochromatic portion of the X is removed from its normal site adjacent to the centromere to a distal site close to the telomere (23, 24). In fixed whole-embryo preparations of these In(1)sc^8 embryos, such as the one displayed in Fig. 8*B*, two large fluorescent masses now appear at the nuclear pole that faces the interior of the embryo (see panel labeled BOTTOM) in about half of the embryos (again, presumably the females). We therefore conclude that interphase nuclei normally contain chromosomes in the same polarized orientation previously described for the anoxic nuclei: centromeres facing the exterior and telomeres facing the yolk.

Studies of whole-embryo preparations of anoxic embryos indicate that, in contrast to other blastoderm nuclei, the pole cell nuclei do not have a consistent orientation with respect to the embryo. However within each pole cell the chromosomes have a polarized orientation—with all of the centromeres at one pole of the nucleus and all of the telomeres at the other pole (data not shown).

Heat and Anoxia Have Similar, but Different, Effects on the Embryonic Nuclei

Anoxia and heat shock have been found to produce some similar effects in *Drosophila* cells (see, for example, references 35 and 36). We have therefore studied the morphology of nuclei from cycle 10–13 embryos that were heat-shocked for 30 min at either 35–37°C or at 40–42°C. We observe that the effects of heat shock resemble those of anoxia: in both cases developmental arrest occurs, accompanied by nuclear swelling and condensation of the chromatin onto the inner face of an intact nuclear envelope. However, in the heat-shocked embryos the condensed chromatin is never observed in the form of linear chromosomes. Instead, the chromatin condenses in a more disorganized fashion, as shown in the cycle 10 nuclei displayed in Fig. 9. A more severe heat shock than that used in the Fig. 9 experiment produces a more extensive aggregation of the chromatin, and in many nuclei detachment of the chromatin from the nuclear envelope occurs (data not shown). Only interphase nuclei and no recognizable prophase, prometaphase, metaphase, anaphase, or telophase nuclei were found in the heat shocked embryos.

We have also examined mid-cycle 14 embryos that were heat-shocked for 30 min, either at 35–37°C or at 40–42°C. Nuclei from embryos that were heat-shocked at 35–37°C appear identical to those of normal cycle 14 nuclei. However, cycle 14 nuclei from embryos heat-shocked at 40–42°C are swollen and contain unusually condensed chromatin.

DISCUSSION

Nuclear Volume as a Function of Nuclear Activity

The syncytial blastoderm stages discussed in this report provide extraordinary material for studies of the nuclear cycle. In a nearly synchronous manner, large numbers of nuclei that are clearly visible at the periphery of the living embryo undergo the most rapid nuclear cycle known in eucaryotes. These nuclei expand and contract rapidly in volume throughout the cycle, while undergoing drastic changes in their chromatin organization.

Sudden nuclear expansions have also been seen in other

[2] Foe, V. Manuscript submitted for publication.

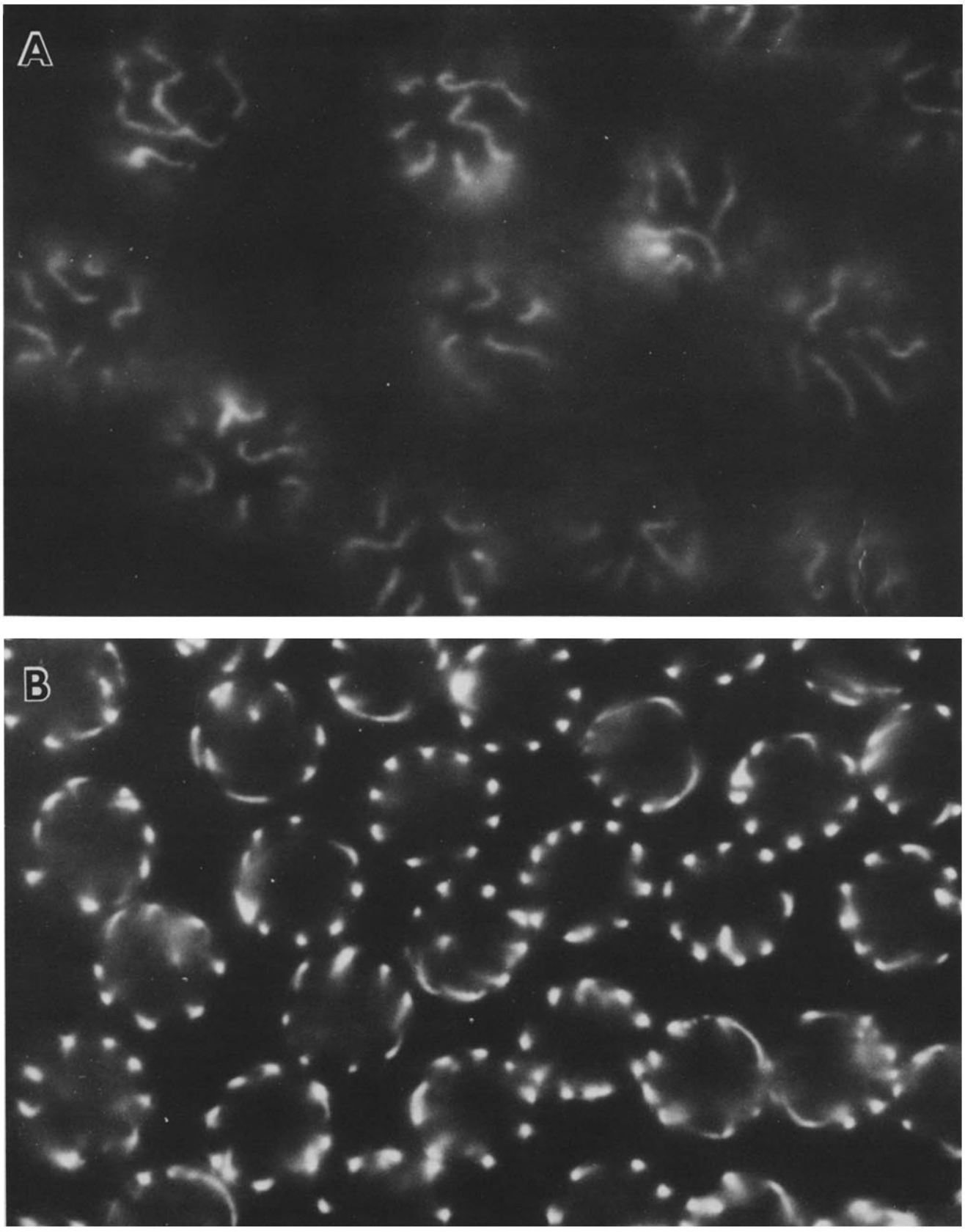

FIGURE 7 The chromosomes in whole-embryo preparations of syncytial blastoderm-stage embryos arrested by oxygen deprivation at prophase. Both micrographs are of the peripherally located, somatic nuclei in an intact, fixed, and stained anoxic embryo. In *A*, a stage 11 embryo, the plane of focus is on the interior-facing pole of the nuclei, revealing that the telomeres are all oriented towards the embryo interior. (The curved surface of the embryo puts the various nuclei at slightly different planes of focus.) In *B* the plane of focus is on the midsection of the nuclei. 8–10 chromosome arms are revealed in each nucleus (10 arms are expected if all chromosome arms extend down the nucleus as far as the plane of focus). The embryo in *B* is at stage 13; comparison of *A* and *B* illustrates the progressively smaller diameter of nuclei arrested in later division cycles (see text and legend to Table II). Note that, as described in Materials and Methods, shrinkage in the whole embryo preparations results in their nuclei having about ⅔ the diameter of analogous nuclei in squash preparations. This shrinkage is also evident in Fig. 8. × 2,600.

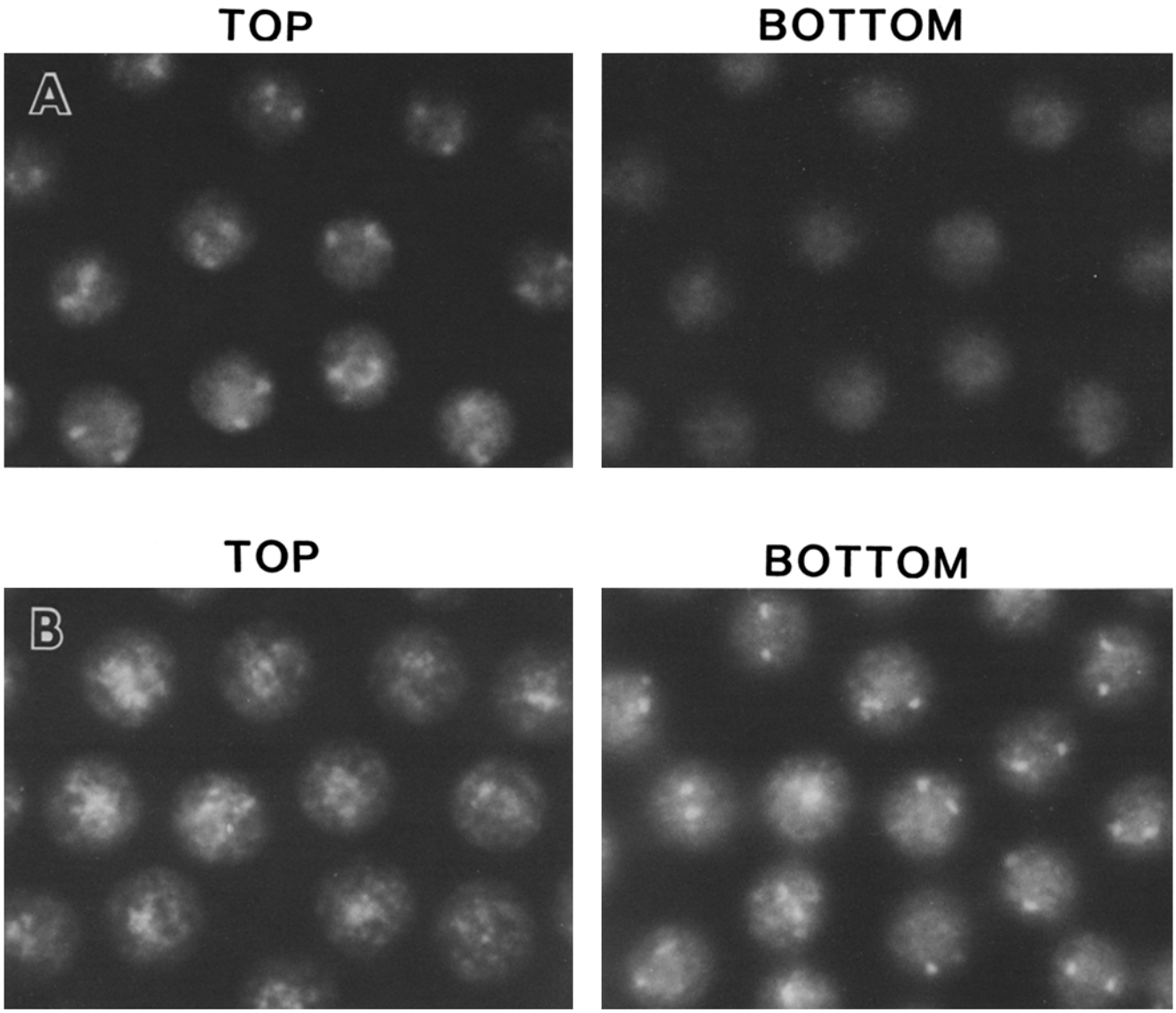

FIGURE 8 Fluorescently stained nuclei in whole-embryo preparations of wild-type and In(1)sc^{8} embryos during cycle 13 interphase. In the panels labeled top, the plane of focus is on the exterior-facing poles of the nuclei, whereas in the righthand panels (*bottom*) the focus is on the nuclear poles that face the yolky interior of the embryo. Here we compare *A*, a wild-type embryo, with *B*, a mutant In(1)sc^{8} embryo, in which the centromere-proximal heterochromatin of the X chromosome has been moved to the X chromosome telomere by an inversion. In the normal embryo, two highly fluorescent patches are visible at the exterior-facing pole, and the interior-facing nuclear pole contains only a diffuse, even fluorescence. In the mutant embryo, it is now the interior-facing nuclear poly (*bottom*) that contains the two highly fluorescent patches; in the mutant embryo the exterior-facing pole is characterized by an irregular, less intense fluorescence that represents the condensation of the centromeric heterochromatin of the autosomes. The embryos shown in both *A* and *B* are inferred to be female, with each of the two fluorescent patches representing the heterochromatic region of an X chromosome (see text; also reference 8). Compared with the embryo in *A*, the embryo in *B* has a larger nuclear volume, a more intense fluorescence, and heterochromatin in a more highly condensed state. It therefore represents a somewhat later phase of interphase than the embryo shown in *A*. × 2,600.

systems, most notably when an inactive nucleus is experimentally transferred into a different cytoplasm that activates it for DNA or RNA synthesis (1, 14, 16, 17). In these cases, inactive nuclei that contain a large amount of condensed chromatin undergo a process of chromatin decondensation accompanying their activation. In several such cases, the nuclear volume has been found to be directly proportional to the rate of RNA synthesis that is induced (16, 17).

In the early *Drosophila* embryos the greatest nuclear volumes occur in those cycles with the shortest interphase times. In fact, the areas under the curves shown in Fig. 2*B* ($\int' V dt$, where t is the length of interphase in each cycle and V is the nuclear volume as a function of time) are the same within experimental error for cycles 10 through 12. This suggests that nuclear volumes may be directly proportional to the instantaneous rate of DNA synthesis during these cycles. In *Drosophila*, there is relatively little RNA synthesis during nuclear cycles 10 through 12 (21, 38), so that it is not unreasonable to propose that during these cycles the rate of DNA synthesis alone determines the pattern of chromatin decondensation, which in turn determines the extent of the nuclear swelling. In this view, the nuclear volume is directly proportional to the amount of chromatin decondensed at any given instant, either for DNA synthesis as in the early *Dro-*

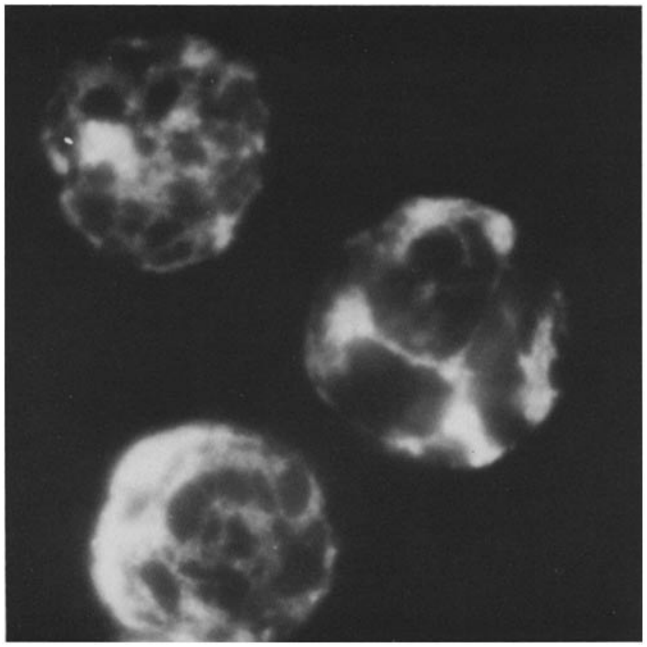

FIGURE 9 The chromatin in heat-shocked syncytial blastoderm nuclei. These nuclei were from a squashed-embryo preparation of an embryo transferred to 37°C saline for 30 min. The embryonic stage was identified as cycle 10 by the morphology of the embryo at the time of squash preparation (see Materials and Methods). See text for description of nuclear morphology.

sophila embryos, or for RNA synthesis as observed in the nuclear transplantation studies (16, 17).

Mechanics of the Nuclear Volume Change

What are the forces that cause the normal interphase nucleus to expand? The decondensation of chromatin could cause the nuclear expansion directly, as the uncoiling DNA presses against the inside of the nuclear envelope. However, the fact that during anoxia the chromosomes condense as the nuclear volume expands means that at least this particular expansion of the nuclear envelope cannot be driven by forces derived from DNA decondensation. Alternatively, it has been suggested that the nuclear expansion could be controlled by osmotic phenomena (18). Osmotic models based on stable osmotic differences are problematic in that they must deal with the difficulty of maintaining any salt gradient across the nuclear pores (for review, see reference 19). However, it is possible that transient osmotic differences generate mechanically stabilized changes in nuclear structure. Transient osmotic disequilibria could be caused by changes in chromatin condensation as well as by other means.

How is the nuclear membrane able to expand so rapidly during anoxia and during normal interphase? Presumably, large quantities of membrane lipids and proteins are readily available due to the continuity of the outer nuclear membrane with the endoplasmic reticulum membrane. It is thought that selected proteins and lipids can rapidly flow from the outer to the inner nuclear membrane around the nuclear pore complexes, where the bilayers of these two nuclear membranes are joined (for review see reference 27). The nuclear lamina, which is thought to form and shape the nucleus by supporting the inner nuclear membrane (13), must likewise be rapidly expandable. The nuclear lamina has very different thicknesses in different cell types (6; see also reference 13), and this structure may consist of multiple layers of the lamina proteins when the nucleus is small that can rapidly expand to form a thinner but more extensive lamina as the nucleus enlarges.

During normal interphase the nuclear envelope expands, apparently to accommodate the decondensing chromatin, whereas during anoxia the envelope expands beyond its normal dimensions at the same time that the chromatin is undergoing a premature recondensation. It is noteworthy that normal nuclei attain their maximum size during mid-interphase, whereas anoxic nuclei reach their maximum size later, during prophase. It is also striking that the size of the anoxic prophase nuclei varies as a function of embryonic stage; in anoxic embryos, the surface area of the prophase nucleus is very close to twofold greater than the maximum area normally attained by the interphase nucleus in the same nuclear cycle (see legend to Table II). By electron microscopy, Stafstrom and Staehelin (34) have observed that a second envelope of similar morphology develops just outside the nuclear envelope before metaphase in normal *Drosophila* embryos. Fusion of the nuclear envelope proper with this second envelope may provide the membrane source that enables the prophase nuclei to double their surface area during anoxia.

Effects of Heat Shock on Nuclear Morphology

It has been shown that anoxia resembles heat shock in inducing the synthesis of the so-called heat-shock proteins in competent tissues (35). This synthesis can occur either during hypoxia or during recovery from total anoxia, but not during total anoxia, apparently due to the depletion during anoxia of the ATP necessary for the transcription and protein synthesis required for the induction of the heat-shock response (22). The heat-shock proteins can be induced in cycle 14 embryos but not in younger embryos (15). Thus, early *Drosophila* embryos provide a natural system in which the morphological consequences of heat shock on nuclei can be compared in the presence and absence of newly synthesized heat-shock proteins.

When syncytial blastoderm embryos of *Drosophila* are shocked by bringing them to ~37°C for 30 min, we find that the nuclei swell as they do during anoxia, and the chromatin condenses. However, linear chromosomes were never observed. Instead, during heat shock the chromatin condenses into disorganized masses, some of which are detached from the nuclear envelope and occupy the nuclear lumen. It is also noteworthy that mitotic nuclei were never observed in the heat-shocked embryos. This indicates that heat shock arrests nuclei only during interphase, whereas anoxia can arrest nuclei at most phases of the cycle. Thus anoxia and heat shock do not have identical effects on nuclei.

Nuclei of midcycle 14 embryos shocked at 35–37°C for 30 min were observed to maintain a normal morphology. This treatment has presumably induced heat-shock proteins. Above 37°C a de novo induction of heat-shock proteins does not occur (35), and we find that treating cycle 14 embryos at 40–42°C for 30 min leads to nuclear swelling and chromatin condensation. Thus, our data suggest that whatever causes the morphologic phenomena of abnormal nuclear swelling and premature chromatin condensation is overcome by the production of the heat-shock proteins.

Effects of Anaerobic Metabolism on Nuclear Morphology

The effect of removing oxygen from developing *Drosophila* embryos was first studied by Zalokar and Erk (39), who noticed both nuclear swelling and a greatly increased number of embryos that contained nuclei "with chromatin threads visible, resembling prophase nuclei." These authors also reported that, after 2 h in an atmosphere of nitrogen, the arrest of development was reversible in 60% of the embryos. Since a similar arrest was obtained when permeabilized embryos were treated with the uncoupler 2,4-dinitrophenol (39), it seems reasonable to attribute the effects seen to the cessation of oxidative phosphorylation expected from both treatments.

Studies carried out with a variety of vertebrate tissues have shown that stopping oxidative phosphorylation causes a large number of different biochemical changes in cells, including rapid increases in NADH, ADP, AMP, and inorganic phosphate levels, and a rapid decrease in the concentration of ATP. There is also a major increase in the lactic acid concentration and a concomitant lowering of the intracellular pH. Many of these changes occur with half-times of 1 min or less and are just as rapidly reversed (see, for example, reference 28). Thus, although one is tempted to ascribe the changes observed in anoxic *Drosophila* embryos to a fall in ATP levels, in actuality any one of a large number of different metabolic changes (or some combination of them) could be causing the reversible changes in nuclear morphology that we have described.

Why does the prematurely condensed interphase chromatin become tightly aligned along an intact nuclear envelope in oxygen-deprived embryos? The result is especially remarkable because it contrasts with the result obtained when mammalian chromatin is prematurely condensed by fusing a cell in interphase with a second cell in mitosis (20). In the latter case, the nuclear envelope apparently disintegrates, just as it does in a normal mitotic cell, as the chromosomes condense. One possible explanation relates to the effect of anoxia on ATP levels. If the ATP-mediated phosphorylation of the nuclear lamina proteins is required for nuclear envelope breakdown during mitosis, as proposed by Gerace and Blobel (12), then one might expect the nuclear envelope to remain intact in anoxic embryos due to a reduced level of ATP, as observed.

As described in detail elsewhere,[2] we believe that the tight membrane attachment of the prematurely condensed chromatin observed in our studies reflects the fact that the chromosomes normally retain numerous points of firm attachment to the nuclear envelope when they decondense during interphase. It is this firm attachment that is postulated to maintain each chromosome in a polarized orientation, with centromeres facing the embryo exterior.

Nuclear Polarity in the Blastoderm Embryo

Electron microscopic examination of sectioned cellular blastoderm *Drosophila* embryos shows a polarized orientation of the nuclei; large electron-dense regions of condensed chromatin occur at the exterior-facing pole of the cycle 14 nuclei (10, 25, 33). Studies on a related dipteran (*Samoania bonensis*) at the cellular blastoderm stage have shown that A:T-rich DNA sequences, which occur predominantly at centromeres, are localized at this exterior-facing nuclear pole (4). The prematurely condensed chromosomes induced in embryos deprived of oxygen provide a direct and dramatic visual confirmation of the inferred polarized orientation of each chromosome in cycle 14 nuclei.[2] The present studies show that this same polar orientation occurs in the interphase nuclei of the earlier syncytial blastoderm stages (cycles 10–13) and that it is retained during the chromatin condensation induced by anoxia.

This orientation of chromosomes with centromeres at one pole and telomeres at the opposite pole has been termed the "Rabl" or "telophase" configuration, and it appears to be common to many eukaryotic cell types (Rabl, 1885 and Boveri, 1888, cited in reference 37; see also literature cited in references 2, 11, and 26). The telophase configuration is so named because it resembles the polarized orientation of the chromosomes as they enter telophase (centromeres pulled forward by the spindle, telomeres trailing behind). In our studies of stained whole embryos, we observe that the telophase configuration is maintained throughout interphase. However, it is striking that, in stained whole embryos, anaphase and telophase nuclei are observed to have their chromosome arms oriented parallel to the embryonic surface (see for example Fig. 8 of reference 7; also reference 5 for similar observations on *Drosophila virilis*) rather than perpendicular to it as observed in the late interphase and prophase nuclei. It is during the telophase to interphase transition, just as they are becoming round, that the nuclei rotate by 90° to adopt their interphase orientation (unpublished results of Dr. Foe; also reported for some other cell types by Wilson [37]).

Ellison and Howard (5), studying Hoechst-stained, sectioned *Drosophila virilis* embryos, observed that the polarized orientation of the interphase nuclei observed in cellular blastoderm embryos is maintained during gastrulation: the invaginating cells are oriented with their more fluorescent (centromeric) poles towards the developing lumen, which topologically is the embryo exterior. The polarity of the individual blastoderm nuclei in the invaginating cell sheet may be retained because the nucleus maintains its orientation with reference to the cell throughout interphase and adjacent blastoderm cells are mechanically bonded together by desmosomelike structures (3, 25, 30). In contrast, we observe that the pole cell nuclei appear to lack a fixed orientation with respect to the embryo; these pole cells are not attached to each other, and during gastrulation they rotate freely (unpublished time-lapse video observations of Dr. Foe).

We thank John Sedat, Tom Kornberg, and Charles Laird for their invaluable advice and Friday Harbor Laboratories for permitting us to make use of their laboratory facilities for part of this work. We also thank Larry Sandler for providing us with the In(1)sc^8 *Drosophila* stock. The skillful assistance of Kathleen Raneses and Leslie Spector in preparing this manuscript is sincerely appreciated.

This work was supported by a grant from the National Institute of General Medical Sciences of the National Institutes of Health to Dr. Alberts and by a Senior Fellowship from the American Cancer Society to Dr. Foe.

Received for publication 16 November 1984, and in revised form 17 January 1985.

REFERENCES

1. Appels, R., P. B. Bell, and N. R. Ringertz. 1975. The first division of HeLa × chick erythrocyte heterokaryons: transfer of chick nuclei to daughter cells. *Exp. Cell Res.* 92:79–86.
2. Comings, D. E. 1968. The rational for an ordered arrangement of chromatin in the

interphase nucleus. *Am. J. Hum. Genet.* 20:440–460.
3. Eichenberger-Glinz, S. 1979. Intercellular junctions during development and in tissue cultures of *Drosophila melanogaster*: an electron-microscopic study. *Wilhelm Roux' Arch. Dev. Biol.* 186:333–349.
4. Ellison, J. R., and H. J. Barr. 1972. Quinacrine fluorescence of specific chromosome regions; late replication and high A:T content in *Samoaia leonensis*. *Chromosoma (Berl.)*. 36:375–390.
5. Ellison, J. R., and G. C. Howard. 1981. Non-random position of the A-T rich DNA sequences in early embryos of *Drosophila virilis*. *Chromosoma (Berl.)*. 83:555–561.
6. Fawcett, D. W. 1981. *In* The Cell. 2nd. Edition. W. B. Saunders, Philadelphia. 281–291.
7. Foe, V., and B. M. Alberts. 1983. Studies of nuclear and cytoplasmic behavior during the five mitotic cycles that precede gastrulation in *Drosophila* embryogenesis. *J. Cell Sci.* 61:31–70.
8. Deleted in press.
9. Fullilove, S. L., and A. G. Jacobson. 1971. Nuclear elongation and cytokinesis in *Drosophila montana*. *Dev. Biol.* 26:560–577.
10. Fullilove, S. L., and A. G. Jacobson. 1978. Descriptive embryonic development. *In* The Genetics and Biology of *Drosophila*. Vol. 2c. M. Ashburner and T. R. F. Wright, editors. Academic Press, Inc., New York. 106–229.
11. Fussell, C. P. 1975. The position of interphase chromosomes and late replicating DNA in centromere and telomere regions of *Allium cepa L. Chromosoma (Berl.)* 50:201–210.
12. Gerace, L., and G. Blobel. 1980. The nuclear envelope lamina is reversibly depolymerized during mitosis. *Cell.* 19:277–287.
13. Gerace, L., A. Blum, and G. Blobel. 1978. Immunocytochemical localization of the major polypeptides of the nuclear pore complex-lamina fraction; interphase and mitotic distribution. *J. Cell Biol.* 79:546–566.
14. Graham, C. F., K. Arms, and J. B. Gurdon. 1966. The induction of DNA synthesis by frog egg cytoplasm. *Dev. Biol.* 14:349–381.
15. Graziosi, G., F. Micali, R. Mazari, F. DeCristini, and A. Savroni. 1980. Variability of response of early *Drosophila* embryos to heat shock. *J. Exp. Zool.* 214:141–145.
16. Gurdon, J. B. 1968. Changes in somatic cell nuclei inserted into growing and maturing amphibian oocytes. *J. Embryol. Exp. Morphol.* 20:401–414.
17. Harris, H. 1967. The reactivation of the red cell nucleus. *J. Cell Sci.* 2:23–32.
18. Harris, H. 1968. Nucleus and Cytoplasm. Clarendon Press, Oxford. 100–103.
19. Horowitz, S. B., and P. L. Paine. 1976. Cytoplasmic exclusion as a basis for asymmetric nucleocytoplasmic solute distributions. *Nature (Lond.)*. 260:151–153.
20. Johnson, R. T., and P. N. Rao. 1970. Mammalian cell fusion. II. Induction of premature chromosome condensation in interphase nuclei. *Nature (Lond.)*. 226:717–722.
21. Lamb, M. M., and C. D. Laird. 1976. Increase in nuclear poly(A)-containing RNA at syncytial blastoderm in Drosophila melanogaster embryos. *Dev. Biol.* 52:31–42.
22. Lewis, M. J., P. J. Helmsing, and M. Ashburner. 1975. Parallel changes in puffing activity and patterns of synthesis in salivary glands of *Drosophila*. *Proc. Natl. Acad. Sci. USA.* 72:3604–3609.
23. Lifschytz, E., and D. Hareven. 1982. Heterochromatin markers: arrangement of obligatory heterochromatin, histone genes and multisite gene families in the interphase nucleus of *D. melanogaster*. *Chromosoma (Berl.)*. 86:443–445.
24. Lindsley, D. L., and E. N. Grell. 1968. Genetic Variations of *Drosophila melanogaster*. Carnegie Institution of Washington, Washington, DC. 330.
25. Mahowald, A. P. 1963. Ultrastructural differentiations during formation of the blastoderm in the *Drosophila melanogaster* embryo. *Dev. Biol.* 8:186–204.
26. Mathog, D., M. Hochstrasser, Y. Gruenbaum, H. Saumweber, and J. Sedat. 1984. Characteristic folding pattern of polytene chromosomes in *Drosophila* salivary gland nuclei. *Nature (Lond.). 308,* 414–421.
27. Maul, G. G. 1977. The nuclear and the cytoplasmic pore complex: structure, dynamics, distribution and evolution. *Int. Rev. Cytol. Suppl.* 6:75–186.
28. McLaughlin, A. C., H. Takeda, and B. Chance. 1979. Rapid ATP assays in perfused mouse liver by ^{31}P NMR. *Proc. Natl. Acad. Sci. USA.* 76:5445–5449.
29. Mitchison, T., and J. Sedat. 1983. Localization of antigenic determinants in whole Drosophila embryos. *Dev. Biol.* 99:261–264.
30. Newman, S. M., Jr., and G. Schubiger. 1980. A morphological and developmental study of *Drosophila* embryos ligated during nuclear multiplication. *Dev. Biol.* 79:128–138.
31. Rabinowitz, M. 1941. Studies on the cytology and early embryology of the egg of Drosophila melanogaster. *J. Morphol.* 69:1–49.
32. Rohme, P. 1975. Evidence suggesting chromosome continuity during S-phase of Indian muntjac cells. *Hereditas.* 80:145–149.
33. Sonnenblick, B. P. 1950. The early embryology of Drosophila melanogaster. *In* The Biology of Drosophila. M. Demerec, editor. Hafner Publishing Company, New York. 52–76.
34. Stafstrom, J. P., and L. A. Staehelin. 1984. Dynamics of the nuclear envelope and of nuclear pores during mitosis in the Drosophila embryo. *Eur. J. Cell Biol.* In press.
35. Velazquez, J. M., and S. Lindquist. 1984. hsp70: Nuclear concentration during environmental stress and cytoplasmic storage during recovery. *Cell.* 36:655–662.
36. Velazquez, J. M., P. J. Helmsing, and M. Ashburner. 1975. Parallel changes in puffing activity and patterns of synthesis in salivary glands of *Drosophila*. *Proc. Natl. Acad. Sci. USA.* 72:3604–3609.
37. Wilson, E. B. 1925. The Cell in Development and Heredity. 3rd Edition. Macmillan Company, New York. 139–140; 890–892.
38. Zalokar, M. 1976. Autoradiographic study of protein and RNA formation during early development of Drosophila eggs. *Dev. Biol.* 49:425–437.
39. Zalokar, M., and I. Erk. 1976. Division and migration of nuclei during early embryogenesis of Drosophila melanogaster. *J. Microsc. Biol. Cell.* 25:97–106.